Parametric Level-Set Full-Waveform Inversion in the Presence of Salt-Bodies

Ajinkya Kadu[*], *Wim A. Mulder*[†], *Tristan van Leeuwen*[*]
[*] *Mathematical Institute, Utrecht University*
[†] *Shell Global Solutions International B.V. & Delft University of Technology*

SUMMARY

Full-waveform inversion attempts to estimate a high-resolution model of the Earth by inverting all the seismic data. This procedure fails if the Earth model contains high-contrast bodies such as salt and if sufficiently low frequencies are absent from the data. Salt bodies are important for hydrocarbon exploration because oil or gas reservoirs are often located on their sides or underneath. We represent the shape of the salt body with a level set, constructed from radial basis functions to keep its dimensionality low. We have shown earlier that the salt body can be completely recovered if the sediment structure is already known. In this paper, we propose a strategy to simultaneously reconstruct the sediment and the salt. The sediment is implicitly represented by a bilinear interpolation kernel with a small number of variables. An alternating minimization technique solves the resulting optimization problem. The results on a synthetic model using Gauss-Newton approximation of the Hessian shows the feasibility of the approach.

INTRODUCTION

Full-waveform inversion (FWI) has become a popular technique to produce high-resolution maps of the subsurface velocity and density from the available seismic data. In its classic form, the method obtains a model by iteratively fitting modeled to observed data in a least-squares sense. Because the underlying minimization problem is highly nonlinear and seismic data typically lack sufficiently low frequencies, a good initial guess of the model is required to avoid convergence to the nearest local minimum, which generally does not represent the ground truth (Virieux and Operto, 2009). The problem becomes worse in the presence of salt bodies, which are of particular interest to the oil industry because hydrocarbon reservoir are often located nearby or underneath. Often, conventional FWI reconstructs the top of the salt but fails to obtain its interior, its bottom, and everything underneath.

A level set can help to regularize the problem. Santosa (1996) introduced the method to geometric inverse problems. It implicitly defines the shape of the salt as the level set or zero contour of a smooth function. The conventional method deals with the level-set evolution through the Hamilton-Jacobi equation, also known as the level-set equation. This approach suffers from steepening and flattening of the level set during iterations. The classic solution, re-initialization of the level set, solves the issue but is computationally intensive. Dahlke et al. (2015), Lewis et al. (2012) and Guo and de Hoop (2013) successfully applied the method in combination with full-waveform inversion.

Previously, we presented a robust implementation that dynamically adapts the width of the level-set boundary to obtain faster convergence (Kadu et al., 2016). This approach implicitly avoids flattening and steepening of level-set function near boundary by adjusting the width according to an approximate level-set gradient. We assumed, however, a known background sediment model. In the present paper, we propose a joint-inversion approach and try to reconstruct the background and salt geometry simultaneously.

THEORY

The FWI problem in its classic least-squares formulation (Tarantola, 1984) reads

$$\min_m \left\{ \tfrac{1}{2} \|F(m) - \mathbf{d}\|_2^2 \right\},$$

where F models the scalar Helmholtz equation, m defines the subsurface model, for instance, P-wave velocity or density or both, and $\mathbf{d}$ represents the data.

It is natural to separate the model into salt and sediment with constant and known salt velocity, m_1 and sediment model m_0:

$$m(\mathbf{x}) = \{1 - a(\mathbf{x})\} m_0(\mathbf{x}) + a(\mathbf{x}) m_1, \tag{1}$$

where a is an indicator function that separates the salt from the sediment. Solving for $a(\mathbf{x})$ is an NP-hard problem because of its discrete nature (Del Lungo and Nivat, 1999). A level-set function, $\phi : \mathbb{R}^2 \to \mathbb{R}$, will simplify the problem:

$$a(\mathbf{x}) = \begin{cases} 1, & \phi(\mathbf{x}) \geq 0; \\ 0, & \phi(\mathbf{x}) < 0. \end{cases}$$

Mathematically, we represent an indicator function with the Heaviside function, i.e., $a(\mathbf{x}) = h(\phi(\mathbf{x}))$. Now, the problem is to find a function $\phi(\mathbf{x})$ that represents the true salt geometry.

Parametric Level-Set Method

Kadu et al. (2016) chose a representation of the level-set function by a linear combination of *finite* compactly-supported radial basis functions (RBFs):

$$\phi(\mathbf{x}) = \sum_{j=1}^{n_s} \alpha_j \psi(\|\mathbf{x} - \boldsymbol{\chi}_j\|_2).$$

Its discrete version is represented by a RBF Kernel Matrix, B, with entries $b_{ij} = [\psi(\|\mathbf{x}_i - \boldsymbol{\chi}_j\|_2)]$, where $\{\mathbf{x}_i\}_{i=1}^n$ represents the model grid points. The RBF nodes $\{\chi_j\}_{j=1}^{n_s}$ are placed on an equidistant model grid. The RBF amplitudes $\{\alpha_j\}_{j=1}^{n_s}$ control the level set. Typically, we use a *sufficiently* smooth Wendland RBF of the form

$$\psi(r) = (1 - r)_+^8 (32r^3 + 25r^2 + 8r + 1).$$

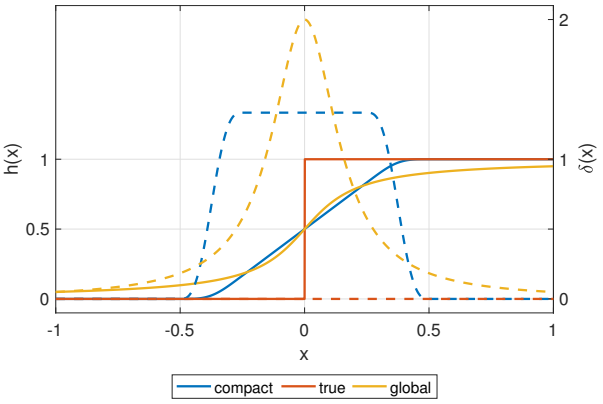

Figure 1: Heaviside and corresponding Dirac-Delta functions (dashed) with a width of 0.5.

The Parametric Level-Set Full-Waveform Inversion (PLS-FWI) for fixed m_0 and m_1 becomes

$$\min_{\boldsymbol{\alpha}\in\mathbb{R}^{ns}} \left\{ f(\boldsymbol{\alpha}) = \tfrac{1}{2}\|F(\boldsymbol{\alpha}) - d\|_2^2 \right\}.$$

The gradient and Gauss-Newton Hessian for this problem are

$$\begin{aligned} g_{\boldsymbol{\alpha}} &= A^T D_{\boldsymbol{\alpha}}^T J^* \left(F(\boldsymbol{\alpha}) - \mathbf{d}\right), \\ H_{\boldsymbol{\alpha}} &= A^T D_{\boldsymbol{\alpha}}^T J^* J D_{\boldsymbol{\alpha}} A, \end{aligned}$$

where J is the Jacobian of the forward modeling operator F. The diagonal matrix $D_{\boldsymbol{\alpha}}$ denotes the element-wise multiplication of the difference between the salt and sediment velocity with the Dirac-Delta function:

$$D_{\boldsymbol{\alpha}} = \mathrm{diag}((m_1 - m_0) \odot h'_{\epsilon}(A\boldsymbol{\alpha})),$$

where $h_{\epsilon}(\cdot)$ is an approximation of the Heaviside function with width ϵ. It is important to note that the level-set sensitivities depend on two main factors: (1) the difference between the salt and sediment velocity and (2) the approximation of the Heaviside function.

We use a compact approximation of the Heaviside function, plotted in Figure 1. This formulation provides a constant region of sensitivity around the level-set boundary. This allows level-set parameters to take large steps as the FWI gradient (i.e., $J^*(F(\boldsymbol{\alpha}) - \mathbf{d})$) are extrapolated by a constant factor. Due to its compactness, only neighboring RBFs are updated, providing less artifacts in the reconstruction.

The width of the Heaviside depends on the level-set boundary and the spatial gradient of the level-set function. Because this gradient is expensive to compute, we approximate it using the lower and upper bounds of level-set function. Hence, the Heaviside width is given by:

$$\begin{aligned} \epsilon &= \kappa \Delta x \left(\frac{\max(\phi) - \min(\phi)}{\Delta x} \right) \\ &= \kappa \left[\max(A\boldsymbol{\alpha}) - \min(A\boldsymbol{\alpha}) \right] \end{aligned} \tag{2}$$

We refer the reader to (Kadu et al., 2017) for more details.

Bilinear Interpolation

We can impose smoothness constraints on the sediment velocity by means of bilinear interpolation from a model on a coarser mesh:

$$m_0(\mathbf{x}) = m_0^{\min} + \sum_{j=1}^{n_b} \beta_j l_j(\mathbf{x} - \widetilde{\boldsymbol{\chi}}_j).$$

Here, $m_0^{\min}$ denotes the water velocity, $l_j(\cdot)$ represents a piecewise linear basis function at node $\widetilde{\boldsymbol{\chi}}_j$ and β_j denotes its corresponding weight. The latter term can be captured using a bilinear interpolation kernel B when the model is discretized on a grid.

For fixed m_1 and $\phi(\mathbf{x})$ in equation (1), the optimization problem becomes

$$\min_{\boldsymbol{\beta}\in\mathbb{R}^{n_b}} f(\boldsymbol{\beta}) = \tfrac{1}{2}\|F(\boldsymbol{\beta}) - \mathbf{d}\|^2.$$

The gradient and Gauss-Newton Hessian are given by

$$\begin{aligned} g_{\boldsymbol{\beta}} &= B^T J^* \left(F(\boldsymbol{\beta}) - \mathbf{d}\right), \\ H_{\boldsymbol{\beta}} &= B^T J^* J B. \end{aligned}$$

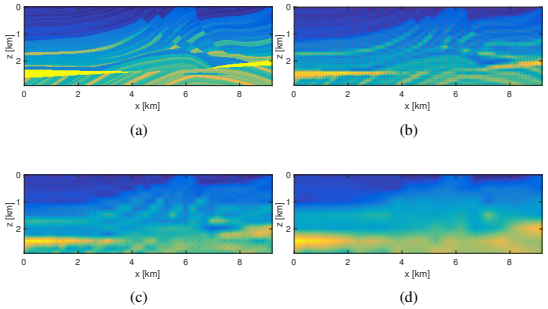

Figure 2: An example of bilinear interpolation. The less nodes, from (a) to (d), the smoother the representation of the model.

Joint reconstruction

The model is now represented in terms of $\boldsymbol{\alpha}$ and $\boldsymbol{\beta}$ as:

$$\mathbf{m} = \{1 - h(A\boldsymbol{\alpha})\} \odot (m_0^{\min} + B\boldsymbol{\beta}) + h(A\boldsymbol{\alpha}) m_1. \tag{3}$$

With prior information about the salt velocity m_1 and water velocity $m_0^{\min}$, the minimization problem becomes

$$\begin{aligned} \min_{\boldsymbol{\alpha},\boldsymbol{\beta}} &\left\{ f(\boldsymbol{\alpha},\boldsymbol{\beta}) = \tfrac{1}{2}\|F(\boldsymbol{\alpha},\boldsymbol{\beta}) - \mathbf{d}\|_2^2 \right\}, \\ &\text{such that } \boldsymbol{\beta}^{\min} \le \boldsymbol{\beta} \le \boldsymbol{\beta}^{\max}. \end{aligned}$$

We use an alternating minimization strategy, splitting the optimization procedure in two parts, namely minimization over the level-set parameters $\boldsymbol{\alpha}$ and minimization over the background parameters $\boldsymbol{\beta}$. We alternately update the level set and the background in a multi-scale fashion. Algorithm 1 presents the basic algorithm, whereas Figure 3 outlines the multi-scale work-flow.

Algorithm 1 Basic Joint Reconstruction Algorithm

Require: **d** - data for frequency batch I_f, F - operator
$m_1, m_0^{\min}, \boldsymbol{\beta}^{\min}, \boldsymbol{\beta}^{\max}$ - model prior information
A, B - Kernel matrices, $\boldsymbol{\alpha}^0, \boldsymbol{\beta}^0$ - initial values
Ensure: $\{\boldsymbol{\alpha}^{\text{final}}, \boldsymbol{\beta}^{\text{final}}\}$, **m** - final model

1: **for** $i = 1$ to $\text{InnerIter}_{\max}$ **do**
2: **for** $j = 1$ to J **do**
3: $\boldsymbol{\beta}^{(j+1)} = \boldsymbol{\beta}^{(j)} + \left(H_{\boldsymbol{\beta}}\left(\boldsymbol{\alpha}^{(i-1)}, \boldsymbol{\beta}^{(j)}\right)\right)^{-1} g_{\boldsymbol{\beta}}\left(\boldsymbol{\alpha}^{(i-1)}, \boldsymbol{\beta}^{(j)}\right)$
4: **end for**
5: $\boldsymbol{\beta}^{(i)} = \boldsymbol{\beta}^{(J)}$
6: **for** $k = 1$ to K **do**
7: $\boldsymbol{\alpha}^{(k+1)} = \boldsymbol{\alpha}^{(k)} + \left(H_{\boldsymbol{\alpha}}\left(\boldsymbol{\alpha}^{(k)}, \boldsymbol{\beta}^{(i)}\right)\right)^{-1} g_{\boldsymbol{\alpha}}\left(\boldsymbol{\alpha}^{(k)}, \boldsymbol{\beta}^{(i)}\right)$
8: **end for**
9: $\boldsymbol{\alpha}^{(i)} = \boldsymbol{\alpha}^{(K)}$
10: **end for**
11: compute **m** from equation (3).

In step 3, we use an interior-point method that incorporates bounds constraints on the parameters $\boldsymbol{\beta}$ and in step 7, a simple Newton method. In both these steps, the descent direction is calculated by a truncated conjugate-gradient method.

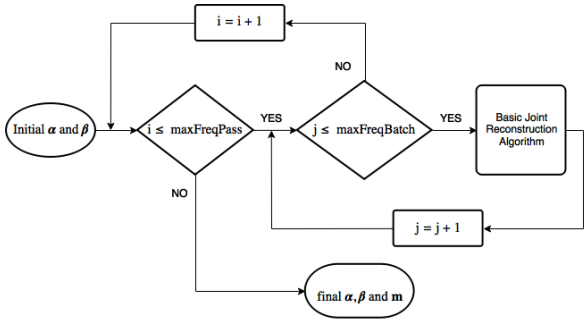

Figure 3: Multiscale Joint Reconstruction Algorithm

Bounds on sediment parameter

To avoid the delineation of salt in the sediment, it is important to put bounds on sediment velocity. Figure 4 shows an example. We allow for smooth updates of the level set near the top region of the salt by constraining the sediment velocity to an upper bound close to true velocity. As noticed in the FWI results, the region just below the top part demands very low velocities. This can also happen with the proposed approach and will slow down the reconstruction procedure. To accelerate the convergence, we impose an appropriate lower bound as a function of *depth*.

EXAMPLES

To demonstrate the capabilities of the proposed method, we present numerical experiments on a synthetic model with acoustic data. Figure 5 shows a model 10 km long and 3 km deep, discretized with a 50-m grid spacing. The sediment is a staircase in depth below a 300-m water layer with velocities between 1500 and 4000 m/s. The salt body, embedded in the sediment, has its top at 200 m below the water bottom with a constant velocity of 4500 m/s. Sources were placed 10 m deep

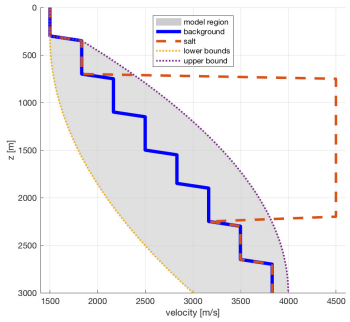

Figure 4: Bounds on the sediment velocity

and 200 m apart. The source is a Ricker wavelet with a 15-Hz peak frequency and zero time lag. The data were acquired with receivers placed 50 m apart starting at a smallest offset of 100 m up to a largest of 4 km. To avoid a full inverse crime, a different finite-difference code generated the data for a model discretized with a much finer grid spacing of 50/8 m. The amplitude of the source wavelet is estimated for each frequency at every step (Pratt, 1999).

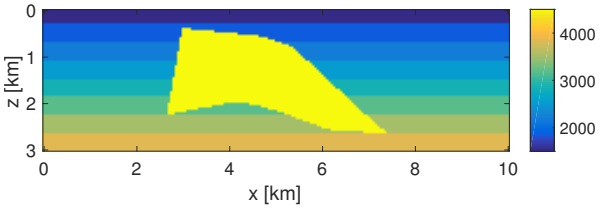

Figure 5: True velocity (in m/s) of synthetic model .

For the classic full-waveform inversion, we apply a spectral projected gradient method with bounds constraints (Schmidt et al., 2009) on the velocity. For the initial model, we take a linear velocity profile with depth. The inversion is performed in a multi-scale fashion over the frequency range 2.5–4.5 Hz with 200 iterations for each frequency batch and a total of 3 passes (Esser et al., 2015) over the frequency range. Figure 6 displays the results. The top of the salt near the water bottom has been reconstructed reasonably well, but not the salt body below. The sediment structure at larger depths is also lost.

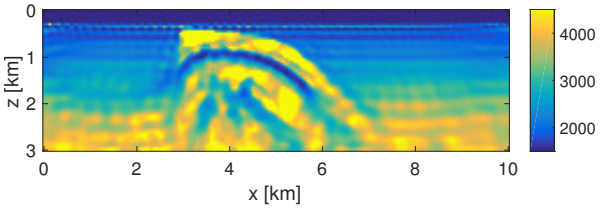

Figure 6: Classic Full-Waveform Inversion results

The parametric level-set parameters $\boldsymbol{\alpha}$ are initialized as shown in Figure 7. All negative RBFs have a value of -1 and all positive of $+1$. We place $25(z) \times 20(x)$ nodes over the model grid for the background. The background parameters $\boldsymbol{\beta}$ are initialized with a smooth linear trend in depth. We incorporate

prior information about the water bottom, at $z = 350$ m, in the initial model.

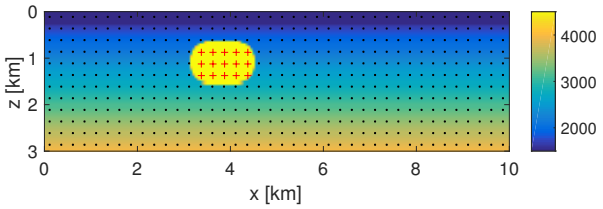

Figure 7: Initial model with velocities in m/s. The level set is initialized around the top of the salt. Positive RBFs are denoted by *red pluses* and negative by *dots*.

The optimization over β is performed with the interior-point method (`fmincon` in MATLAB®). We restrict ourselves to $J = 10$ iterations in algorithm 1. We apply the `minFunc` (Schmidt, 2012) code in MATLAB® to optimize over α, limited to $K = 20$ iterations. In both these steps, the step direction is calculated by at most 10 iterations of the conjugate gradient method. A total of 4 passes are made over the frequency range, along with 2 inner iterations for each frequency batch. In total, we perform about 960 iterations. The Heaviside width parameter (κ) is initialized with 0.05 and reduced by 20% after each frequency pass to produce sharp boundaries for the salt.

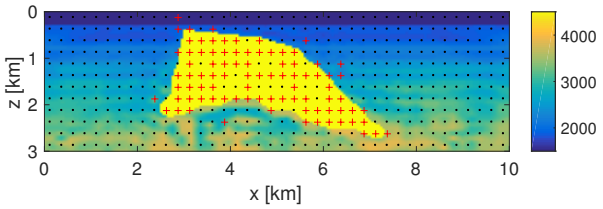

Figure 8: Model obtained by the joint reconstruction approach. Corresponding positive (*pluses*) and negative (*dots*) RBFs.

Figure 8 shows the model obtained with the proposed method. The salt is reconstructed accurately at its top and sides. The sediment structure is reconstructed well down to a depth of 1.5 km as shown in Figure 10. Figure 9 illustrates the need for multiple passes over the frequency range. Figure 11 shows that the method manages to fit the data for the lower frequencies but not for the higher.

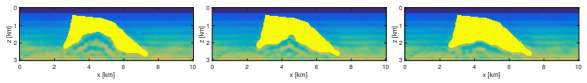

(a) (b) (c)

Figure 9: Reconstructed model after the 1st (a), 2nd (b) and 3rd (c) frequency pass.

CONCLUSIONS

We have proposed a joint reconstruction approach for salt delineation in seismic full-waveform inversion. Our approach is based on the idea of separating the model into salt and sediment. The salt geometry is defined with a level set represented by radial basis functions. The sediment, in turn, is represented by piecewise linear functions on a small number of nodes. This low-dimensional formulation of the model imposes smoothness on the sediment and on the salt geometries. The proposed compact approximation of the Heaviside function leads to faster convergence and produces no artifacts. We apply an alternating minimization strategy to optimize over the two different parameters. Results on a synthetic acoustic example demonstrates the method's capability. The proposed method accurately predicts the salt geometry where the conventional full-waveform inversion fails.

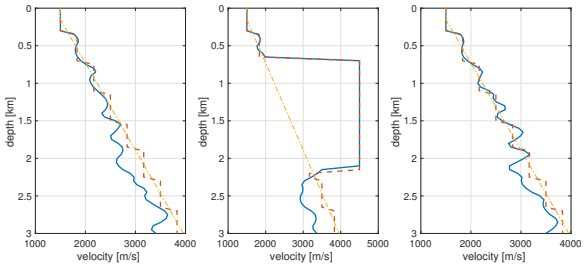

(a) (b) (c)

Figure 10: Velocity profile at $x = 2$ km (a), $x = 5$ km (b), and $x = 8$ km (c). The *blue* line denotes the reconstructed velocity, the *red dotted* line denotes the true velocity, while the *yellow dash-dotted* line represents the initial velocity.

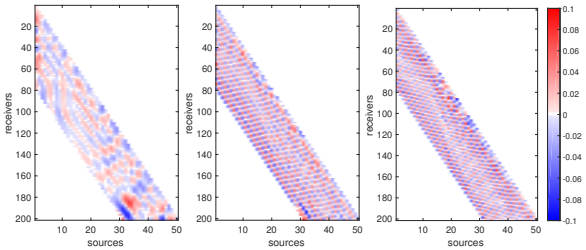

(a) (b) (c)

Figure 11: Normalized data misfit (only *real* part) for final reconstructed model at (a) 2.5 Hz, (b) 3.5 Hz, and (c) 4.5 Hz. We normalized the differences by the maximum value of the true data per frequency.

ACKNOWLEDGMENT

This work is part of the Industrial Partnership Programme (IPP) 'Computational sciences for energy research' of the Foundation for Fundamental Research on Matter (FOM), which is part of the Netherlands Organisation for Scientific Research (NWO). This research programme is co-financed by Shell Global Solutions International B.V. The third author is financially supported by the Netherlands Organisation for Scientific Research (NWO) as part of research programme 613.009.032. We acknowledge Seismic Laboratory for Modeling and Imaging (SLIM) at UBC for providing computational software.

REFERENCES

Dahlke, T., B. Biondi, and R. Clapp, 2015, Domain decomposition of level set updates for salt segmentation, *in* SEG Technical Program Expanded Abstracts 2015: Society of Exploration Geophysicists, 1366–1371.

Del Lungo, A., and M. Nivat, 1999, Reconstruction of connected sets from two projections, *in* Discrete tomography: Springer, 163–188.

Esser, E., L. Guasch, T. van Leeuwen, A. Y. Aravkin, and F. J. Herrmann, 2015, Automatic salt delineation – wavefield reconstruction inversion with convex constraints, *in* SEG Technical Program Expanded Abstracts 2015: Society of Exploration Geophysicists, 1337–1343.

Guo, Z., and M. V. de Hoop, 2013, Shape optimization and level set method in full waveform inversion with 3D body reconstruction, *in* SEG Technical Program Expanded Abstracts 2013: Society of Exploration Geophysicists, 1079–1083.

Kadu, A., T. van Leeuwen, and W. A. Mulder, 2016, A parametric level-set approach for seismic full-waveform inversion, *in* SEG Technical Program Expanded Abstracts 2016: Society of Exploration Geophysicists, 1146–1150.

———, 2017, Salt reconstruction in full waveform inversion with a parametric level-set method: IEEE Transactions on Computational Imaging, **3**, 1–11.

Lewis, W., B. Starr, and D. Vigh, 2012, A level set approach to salt geometry inversion in full-waveform inversion, *in* SEG Technical Program Expanded Abstracts 2012: Society of Exploration Geophysicists, 1–5.

Pratt, R. G., 1999, Seismic waveform inversion in the frequency domain, part 1: Theory and verification in a physical scale model: Geophysics, **64**, 888–901.

Santosa, F., 1996, A level-set approach for inverse problems involving obstacles: ESAIM: Control, Optimisation and Calculus of Variations, **1**, 17–33.

Schmidt, M., 2012, minfunc: unconstrained differentiable multivariate optimization in matlab: URL http://www. di. ens. fr/mschmidt/Software/minFunc. html.

Schmidt, M. W., E. van den Berg, M. P. Friedlander, and K. P. Murphy, 2009, Optimizing costly functions with simple constraints: A limited-memory projected quasi-newton algorithm.: AISTATS, 456–463.

Tarantola, A., 1984, Inversion of seismic reflection data in the acoustic approximation: Geophysics, **49**, 1259–1266.

Virieux, J., and S. Operto, 2009, An overview of full-waveform inversion in exploration geophysics: Geophysics, **74**, WCC1–WCC26.